Age-Optimal Mobile Elements Scheduling for Recharging and Data Collection in Green IoT

JIANXIN MA [1], **SHUO SHI** [1,2], **(Member, IEEE), SHUSHI GU** [2,3], **(Member, IEEE),**
NING ZHANG [4], **(Senior Member, IEEE), AND XUEMAI GU** [1,2]

[1]Department of Electrical and Information Engineering, Harbin Institute of Technology, Harbin 150001, China
[2]Network Communication Research Centre, Peng Cheng Laboratory, Shenzhen 518052, China
[3]School of Electronic and Information Engineering, Harbin Institute of Technology (Shenzhen), Shenzhen 518055, China
[4]Department of Computing Sciences, Texas A&M University-Corpus Christi, Corpus Christi, TX 78412, USA

Corresponding author: Shuo Shi (crcss@hit.edu.cn)

ABSTRACT Ensuring real-time reporting of fresh information and maintaining the sustainability of power supply is of great importance in time-critical green Internet of Things (IoT). In this paper, we investigate the mobile element scheduling problem in a network with multiple independent and rechargeable sensors, in which mobile elements are dispatched to collect data packets from the sensor nodes and to recharge them. The age of information (AoI) is used to measure the time elapsed of the most recently delivered packet since the generation of the packet. We propose an age-optimal mobile elements scheduling (AMES), which decides the trajectories of mobile elements based on a cooperative enforcement game and completes the time-slot allocation in each meeting point, to minimize the average AoI and maximize the energy efficiency. The cooperative enforcement game enables the mobile elements to make optimal visiting decisions and avoid the visiting conflicts, and the outcome of the game is pareto-optimal. Compared to the existing approaches, i.e., greedy algorithm (GA), greedy-neighborhood algorithm (GA-neighborhood), simulation results demonstrate that AMES can achieve a lower average AoI and a higher energy efficiency with a higher successful visiting ratio of the sensor node.

INDEX TERMS Mobile element scheduling, data collection, age of information, energy efficiency, green IoT.

I. INTRODUCTION

Green Internet of Things (IoT) typically consists of a large number of low-cost and small-size wireless sensors [1], [2]. Traditionally, sensors measure and monitor ambient conditions in the surrounding environment and then send the measurements and monitored information to a static sink [3]. However, due to the limited capacity of sensors, maintaining sustainable energy supply of sensors becomes a major research challenge [4], [5]. With the development of wireless energy transfer technology, the sink as an energy source can transfer energy to sensors [6]. Due to the limitation of coverage area of the sink, the mobile elements, i.e, vehicles, robots and UAVs, have been widely employed to collect the information from sensors and charge the sensors as a

relay [7], [8]. With such a great potential, using multiple such mobile elements to collect data and charge sensors has become a promising solution in some application services, i.e, smart cities, public security, critical infrastructure protection and so on [9], [10].

With the rapid growth of the diversity of IoT applications and mobile data traffic, the demands for the freshness of information and energy efficiency has dramatically increased in recent years. The Age of Information (AoI) is a performance metric that measures the time elapsed since the generation of the data packet [11], which can capture the freshness of information from the perspective of the destination. For the applications that generate time-sensitive information such as position, command and control [12], the transmission scheduling policies play an important role in minimizing AoI. In the literature, some works design the transmission scheduling policies in a single-hop wireless network, where

The associate editor coordinating the review of this manuscript and approving it for publication was Nan Cheng.

sensors directly transmit time-sensitive information to a base station [13], [14]. The multi-hop networks are also considered and studied [15], [16]. the sensor nodes can transmit real-time data packets and harvest energy from radio frequency signals to deal with the age of information [17], [18]. Although these works consider the energy harvesting technology, they only focus on the single-hop or the multiple-hop situation without considering mobile elements.

In addition to the transmission scheduling policies, mobile elements' trajectories also have a great impact on AoI and energy efficiency in relay-based green IoT. Moreover, task scheduling for mobile elements can further reduce the average AoI and improve energy efficiency [19], [20]. In many practical applications, the mobile elements cannot predict the information of sensor nodes such as network topology and energy consumption rate in advance [21]. Sensor nodes have to send their energy demand or the information transmission requests once they need energy supply or detect effective information [22], [23]. If a mobile element is within its communication range, the mobile element will receive the request and put it into the list of all requests and select the best next candidate to visit.

As we consider the on-line case, the visiting decision of every meeting point will affect the trajectories of mobile elements. In order to maximize energy efficiency, various on-line charging scheduling algorithms are designed [24], [25]. A Linear Programming (LP) for the problem of scheduling a mobile charger is formulated in [26], and an efficient solution based on the gravitational search algorithm (GSA) is proposed. The work in [27] jointly optimizes SNs-UAV scheduling, power allocation strategy and flight trajectory of the UAV. It aims to minimize the total power consumption of the UAV to maximize the required transmission rate. To minimize AoI, in [28], two age-optimal trajectories are designed for UAV-enabled wireless sensor networks in an off-line case, which aims to minimize the age of the 'oldest' sensed information among the sensor nodes (SNs) and the average AoI of all the SNs respectively when a UAV directly collects data from the ground sensor nodes. In contrast with the full charging model, some researchers prefer the partial-charging model as a more effective and flexible model. Reference [29] proposes a schedulability evaluation mechanism for such partial-charging scheduling based on the on-line charging case. However, very few of them consider both the energy requestion and the data transmission requestion for the on-line case.

In this paper, to address the aforementioned problems of mobile elements scheduling in green IoT scenario, we propose an age-optimal mobile elements scheduling (AMES) scheme, in which each meeting point is decided by our delicately designed cooperative enforcement game. In the game, each mobile element as a player chooses the next meeting point of its strategy set after visiting a meeting point. The strategy set is updated in real-time. In order to reduce the average AoI, and to increase the energy efficiency and the successful visiting ratio, only the requesting sensor node

can be added to the strategy set and visited. By following the rules of the game, the meeting points are chosen without the conflicts between mobile elements, and the maximum profits are obtained. The main contributions of this work can be summarized as follows.

- In order to meet the growing demands for the fresh of information and the energy efficiency in green IoT, we formulate the mobile elements scheduling problem as a multi-objective optimization problem. By optimizing the trajectories scheduling of mobile elements, it can minimize the average AoI and maximize the energy efficiency in an online manner.
- We propose an age-optimal mobile elements scheduling scheme, in which the visiting conflict between mobile elements in each decision period is avoided by delicately designing the rules of the cooperative enforcement game. Thus, a sensor node will not be visited by more than one mobile element in the same requesting period, and the mobile elements will visit the requesting sensor nodes in less time and return earlier. The travel distance, travel time and the corresponding energy consumption of the information transmission can be dramatically reduced. Meanwhile, AoI, energy efficiency and the successful visiting ratio can be significantly improved.
- To further reduce the travel time and to reduce the average AoI, the visiting decision-making of mobile elements not only considers the profit of the requesting sensor nodes, but also the one of the sensor's neighbors in our AMES scheme. Based on this, we design the payoff function of the game.
- By comparing with the greedy algorithm (GA) and the greedy-neighborhood algorithm (GA-neighborhood), the simulation results demonstrate that AMES can avoid the visiting conflict, reduce the average AoI, improve the energy efficiency and enhance the successful visiting ratio in the network with multiple independent and rechargeable sensors.

The remainder of this paper is organized as follows. Section II formulates the multi-objective optimization problem. The major contributions are introduced in Section III, which proposes an age-optimal multiple mobile elements scheduling scheme to solve the proposed problem. Section IV analyzes and compares the results of our approach with numerical existing approaches. Finally, Section V concludes this paper. The key symbols used in this paper are summarized in Table 1.

II. PRELIMINARY AND PROBLEM STATEMENT
A. NETWORK MODEL

As shown in Figure 1, we assume that N sensor nodes are randomly deployed in a region $\mathcal{R}$, which are denoted by $\{i, \ i \in 1, \ 2, \ \ldots \ N\}$. The locations of sensors are unknown in advance. Each of them has a fixed communication range that is a circular area with radius r and a unique
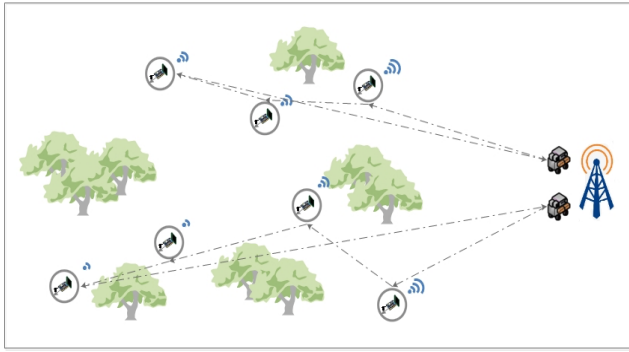
FIGURE 1. Demonstration of mobile elements movements.

TABLE 1. Symbols and definitions.

Symbols	Definitions
N	number of sensors.
M	number of mobile elements.
$X_i(t)$	age of information associated with sensor node i at time t.
ι_i	generation time of the data packet of sensor node i.
$\mathcal{N}_{neighbors_i}$	number of requesting neighbors of sensor node i.
Δ_ξ	decision time after the mobile element j visited the last meeting point $\xi - 1$.
v_j	movement speed of mobile element j.
$\mathcal{N}_j$	number of visited meeting points of the mobile elements j in a round.
π_j^ξ	time-slot allocation strategy of meeting point ξ.
μ	trajectoies scheduling strategy.
E^s	battery capacity of a sensor node.
E^m	battery capacity of a mobile element.
c_s	sensing energy consumption rate.
$E_i^{s_r}(t)$	residual energy of the sensor node i at t.
$E_j^{m_r}$	residual energy of the mobile element j.

identification (ID). When a sensor node generates a new packet, or when its power is lower than the threshold, the request signal will be broadcasted to mobile elements.

There are M mobile elements out of the region $\mathcal{R}$, which are indicated by $\{j, j \in 1, 2, \ldots M\}$. These mobile elements collect data from the sensor nodes and recharge the sensor nodes. The mobile elements depart from the sink point and serve the sensor nodes in a cyclic fashion, respectively. In each period, when the condition is satisfied, the mobile element will return to the sink point. Based on the trajectories of mobile elements, AoI can be calculated in the following section.

B. AGE OF INFORMATION

At time ι_i, the sensor node i generates a data packet and requests to send it to the mobile element. We use $X_i(t)$ to track the age of information collected from the sensor node i in the traveling trajectory at time t, which can be calculated as follows:

$$\begin{cases} X_i(t) = t - \iota_i, & \text{if } t > \iota_i; \\ X_i(t) = 0, & \text{otherwise.} \end{cases} \quad (1)$$

Figure 2 shows an example of the AoI process for a sensor node, in which a_1 is the arrival time of the packet generated
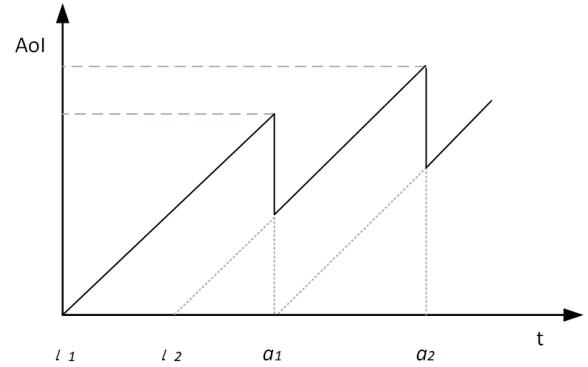

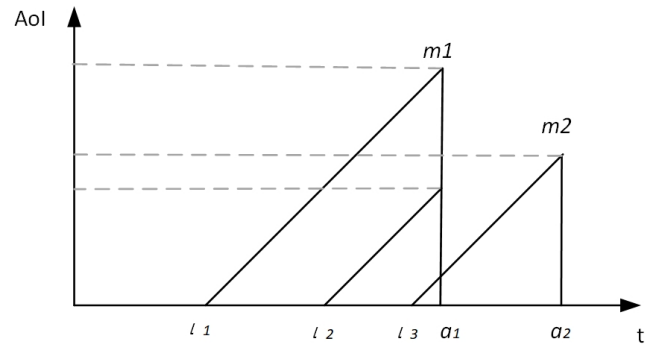**FIGURE 2.** Sample path of the age process at a sensor node.

FIGURE 3. Sample path of the age process at multiple sensor nodes for multiple mobile elements.

at time ι_1 and a_2 is the arrival time of the packet generated at time ι_2. Both two packets are generated by sensor node i, but they are collected in two rounds, respectively. Figure 3 shows an example of multiple AoI processes from three sensor nodes to two mobile elements. ι_1, ι_2 and ι_3 are the generation time of the data packets from sensor nodes 1, 2 and 3. The mobile element 1 as a relay collects the data packets from sensor nodes 1 and 2 to the sink point, and the mobile element 2 as a relay collects the data packet from sensor node 3 to the sink point.

When a mobile element j stops at a meeting point ξ, it does not only visits this meeting point's sensor node, but also the meeting point's neighbors. We will define the neighbors in the following section. We consider a time-slotted system to complete the visiting of each meeting point, which is $\{\sigma_k^{\xi,j}, k \in 1, 2, \ldots \mathcal{N}_{neighbors_\xi}\}$. Then, at slot $\sigma_k^{\xi,j}$, the information age of sensor node i is given by

$$\begin{cases} X_i(\sigma_k^{\xi,j}) = \sigma_k^{\xi,j} - \iota_i, & \text{if } \sigma_k^{\xi,j} > \iota_i; \\ X_i(\sigma_k^{\xi,j}) = 0, & \text{otherwise.} \end{cases} \quad (2)$$

When the mobile element j collected overall sensing information of meeting point ξ, we have

$$\sigma_{\mathcal{N}_{neighbors_\xi}+1}^{\xi,j} = \sigma_1^{\xi,j} + \sum_{k=1}^{\mathcal{N}_{neighbors_\xi}} t_k^{tx}, \quad (3)$$

where $\sum_{k=1}^{\mathcal{N}_{neighbors_\xi}} t_k^{tx}$ is the total time for data transmission and charging at this meeting point. At this time, the information age of sensor node i is given by

$$
\begin{cases}
X_i(\sigma_{\mathcal{N}_{neighbors_\xi}+1}^{\xi,j}) = \sigma_1^{\xi,j} + \sum_{k=1}^{\mathcal{N}_{neighbors_\xi}} t_k^{tx} - \iota_i, \\
\quad \text{if } \sigma_{\mathcal{N}_{neighbors_\xi}+1}^{\xi,j} > \iota_i; \\
X_i(\sigma_{\mathcal{N}_{neighbors_\xi}+1}^{\xi,j}) = 0, \quad \text{otherwise.}
\end{cases}
\tag{4}
$$

The beginning time of the mobile element j to choose each meeting points is assumed as $\{T_\xi^j, \ \xi \ \in \ 1, \ 2, \ \dots \ \mathcal{N}_j\}$. We define

$$
T_{\xi+1}^j = \sigma_{\mathcal{N}_{neighbors_\xi}+1}^{\xi,j}.
\tag{5}
$$

Then, after visiting the meeting point ξ, the information age of the sensor node i is given by

$$
\begin{cases}
X_i(T_{\xi+1}^j) = T_\xi^j + t_{\xi-1,\xi}^v + \Delta_\xi + \sum_{k=1}^{\mathcal{N}_{neighbors_\xi}} t_k^{tx} - \iota_i, \\
\quad \text{if } T_{\xi+1}^j > \iota_i; \\
X_i(T_{\xi+1}^j) = 0, \quad \text{otherwise.}
\end{cases}
\tag{6}
$$

Δ_ξ denotes the decision time after the mobile element j visited the meeting point $\xi - 1$. $t_{\xi-1,\xi}^v$ is the travel time of mobile element j from the meeting point $\xi - 1$ to the meeting point ξ. We assume each pair of travel distance is the straight-line $d_{\xi-1,\xi}$ between these two points, and the mobile element j moves at a constant speed v_j. Thus, the travel time is given by

$$
t_{\xi-1,\xi}^v = d_{\xi-1,\xi}/v_j.
\tag{7}
$$

Here, T_ξ^j is associated with the trajectory of mobile element j, and $\sigma_k^{\xi,j}$ is associated with the time-slot allocation in meeting point ξ.

C. PROBLEM STATEMENT

We assume mobile elements depart from the sink point at time $T_0 = 0$. To collect data, the trajectories scheduling of mobile elements is based on the decision of meeting points. Each meeting point is selected from the requesting sensor nodes in real-time. If a mobile element receives more than one request from multiple sensor nodes in a decision-making process, it needs to decide which is the next meeting point to visit.

As mentioned above, AoI mainly includes the waiting time, the data uploading time and the time elapsed from the sensor node to the sink point. Thus, the average AoI based on the trajectories scheduling scheme μ can be calculated as Equation (8). In Equation (8c), μ_j denotes the trajectory scheduling scheme of the mobile element j, and $X_\xi^j(u_j)$ denotes the total ages of information collected at meeting point ξ. In Equation (8d), the time-slot allocation strategy π_j^ξ of meeting points is considered to improve the successful visiting ratio and the survival ratio of sensor nodes. $\mathcal{N}_j$ denotes the number of meeting points, which is chosen by the mobile elements j

in a round, and $\mathcal{N}_{neighbors_\xi}$ indicates the number of neighbors of the meeting point ξ.

$$
\bar{X}(u), \tag{8a}
$$

$$
= \frac{1}{N} \sum_{i=1}^{N} X_i(u), \tag{8b}
$$

$$
= \frac{1}{N} \sum_{j=1}^{M} \sum_{\xi=1}^{\mathcal{N}_j} X_\xi^j(u_j), \tag{8c}
$$

$$
= \frac{1}{N} \sum_{j=1}^{M} \sum_{\xi=1}^{\mathcal{N}_j} \sum_{k=1}^{\mathcal{N}_{neighbors_\xi}} X_k^\xi(\pi_j^\xi), \tag{8d}
$$

We use E^s and E^m to represent the battery capacity of a sensor node and a mobile element, respectively. $E_i^{s_r}(t)$ denotes the residual energy of the sensor node i at time t. When the residual energy is lower than the threshold, the sensor node sends a charging request. Besides, a sensor node is charged when it transmits data to a mobile element. When a mobile element arrives at a meeting point, all the requesting neighbors of this point directly transmit data to the mobile element by wireless transfer technology. According to [30], to deliver an l-bit message over the distance of $d_{i,\xi}$ the energy consumption of sensor node i in ξ-th meeting point will be

$$
c_t(l, d_{i,\xi}) = E_{tx-elec(l)} + E_{tx-amp(l,d_{i,\xi})} = lE_{elec} + l\varepsilon fs d_{i,\xi}^\alpha,
\tag{9}
$$

where $d_{i,\xi}$ is the transmission distance between the sensor node i and the mobile element ξ. α is the path loss exponent [31]. Besides the transmission consumption, sensing the target also consumes the energy of the sensor node. We use $\tau_i c_s$ to denote the sensing energy consumption, where τ_i denotes the visiting time since the sensor is chosen by a mobile element and c_s denotes the sensing energy consumption rate of per second. Thus, the energy consumption of sensor nodes when it is visited by a mobile element is

$$
c^v(i) = c_t(l, d_{i,\xi}) + \tau_i c_s.
\tag{10}
$$

The sensor node i request $E_i^{request}$ energy from the target mobile element, which is shown as follows:

$$
E_i^{request} = E^s - E_i^{s_r}(t) + c^v(i).
\tag{11}
$$

The total energy obtained by sensor nodes can be calculated as follows:

$$
E_{sc} = \sum_{i=1}^{N} E_i^{request}.
\tag{12}
$$

$E_j^{m_r}$ denotes the residual energy of the mobile element j. The total energy consumed by all the mobile elements is:

$$
E_{mc} = \sum_{j=1}^{M} (E^m - E_j^{m_r}).
\tag{13}
$$

In order to obtain the minimum average AoI and maximum energy efficiency, we formulate a multi-objective optimization problem as follows:

$$\underset{u}{\text{minimize}} \quad \bar{X}(u), \tag{14}$$

$$\underset{u}{\text{maximize}} \quad \eta = \frac{E_{sc}}{E_{mc}}, \tag{15}$$

$$\text{subject to} \quad (d_{j,i} + d_{i,o})\delta_j/v_j \le E_j^{m_r} - E_{i,j}^c, \tag{16}$$

$$c^v(i) < \tau_i\varphi_i \tag{17}$$

Equation (16) is the bound constraint, which guarantees the mobile element j will have enough energy to return to the sink point if it visits the sensor nodes i. δ_j denotes the moving energy consumption rate of the mobile element. $E_{i,j}^c$ denotes the energy consumption of mobile element j if it visits the sensor node i. The average energy replenishment rate of sensor node i in the charging process is denoted by φ_i. Equation (17) is another bound constraint, which ensures the energy replenishment rate is much larger than the energy consumption rate for every visiting.

III. THE PROPOSED AMES SCHEME

In the previous section, we proposed a multi-objective optimization problem to optimize the age of collected information and improve the network energy efficiency. For multi-objective optimization problems, due to the contradiction and non-commensurable of multiple objectives, it is impossible to achieve the optimal solutions for all objectives. We propose AMES scheme to obtain a pareto solution. Except for the sink point, the trajectory is supposed to contain the sequence of the meeting points. In each step of the scheduling process, a mobile element may receive multiple requests and has its own strategy set. Due to the requests of the sensor nodes update at any time and it is also related to the current location of the mobile element, the strategy set is different in each decision. Besides, there are conflicts between mobile elements to obtain the visiting rights of sensor nodes, in which each mobile element wants to visit the sensor node that can obtain the most profit. Therefore, we design a cooperative enforcement game to deal with this conflict and make the visiting decision. Based on the transmission and energy request of each requested sensor node, we design the game strategy as follows.

A. BASIC ELEMENT OF GAME

Game theory contains three basic elements: players, strategy set, and payoff functions. In this work, the game theory model is built for formalizing the visiting decision-making process. Each mobile element is regarded as a player, involving in the game process. For each player, it owns a strategy set S_j which contains all possible actions for it to choose and guide its future movement. The strategy chosen by mobile element j is represented by s_j. Thus, the strategy chosen by all the mobile elements are denoted by a strategy profile $s = \{s_1, s_2, \dots, s_M\}$. Based on the strategy

---

Algorithm 1 Game Process

Input:
    Mobile elements.

Output:
    The best strategy profile s^*.

1: **for** $j = 1; j \le M; j++$ **do**
2:     **for** $i = 1; i \le N; i++$ **do**
3:         **if** sensor node i within the communication range of mobile element j and send a request **then**
4:             $S_j \leftarrow S_j \cup \{i\}$;
5:         **end if**
6:         **for** all $s_k^j \in S_j$ **do**
7:             Calculate the payoff value according to Equation (19);
8:         **end for**
9:     **end for**
10:     Find the optimization solution of mobile element j.
11: **end for**
12: **if** the conflicts are existing between mobile elements **then**
13:     Find a strategy profile s^* that can bring the maximum total profits.
14: **end if**
    return s^*.

---

set, the decision is made by considering the payoff of each action. The payoff is denoted by $P_j(s_j, s_{-j})$ where $s_{-j} = \{s_1, \dots, s_{j-1}, s_{j+1}, \dots, s_M\}$ indicates all other mobile element's strategies except j.

B. GAME THEORY PROCESS

Based on the on-line case, the location and energy consumption rate of sensor nodes cannot be predicted. In the game process, cooperative games cannot be completed among mobile elements, and mobile elements tread to act selfishly. However, when more than one mobile element chooses the same sensor node as the meeting point, the sensor node knowns all the payoff information of them. Based on these information and the designed rules, the sensor node enforces the mobile elements to make the cooperative decisions to maximize the total payoff.

For each mobile element, after visited a meeting point, it needs to choose the next meeting point in the new strategy set. The strategy set contains all the requesting sensor nodes within the communication range when the mobile element is making the decision. In the process of a game, the payoff function is used to constrain the player's behavior. As mentioned above, we use $P_j(s_j, s_{-j})$ to represent the payoff of mobile element j if it chooses the strategy s_j. The payoff of the mobile element is a value that is used to indicate the increase or decrease of the profit, which can be increased or decreased.

The energy consumption for traveling is the loss of profits and the energy for charging the sensor node makes

a profit. Similarly, that the data packet is received by the mobile element makes profits. The moving energy consumption is related to the distance between the mobile element j and the sensor node i, and the distance can be calculated as

$$d_{j,i} = \sqrt{(x_j - x_i)^2 + (y_j - y_i)^2}, \qquad (18)$$

where the location of the mobile element j is represented by its coordinate (x_j, y_j) in the two-dimensional space, and the location of the sensor node i is represented by (x_i, y_i) in the two-dimensional space.

The battery capacity of a mobile element is much larger than the battery capacity of a sensor node. Even so, the mobile element requests enough energy to return after completed the visiting tasks. Thus, we design our payoff function as follows:

$$P_j(s_j, s_{-j}) = \frac{\sum_{k=1}^{\mathcal{N}_{neighbors_{\xi_{s_j}}}} (E^s - E_k^{s_r}(t) + c^v(k) + X_k(t))}{d_{j,i}}, \qquad (19)$$

where $\sum_{k=1}^{\mathcal{N}_{neighbors_{\xi_{s_j}}}} (E^s - E_k^{s_r}(t) + c^v(k))$ denotes the energy that all the neighbors obtain in strategy s_j. $\sum_{k=1}^{\mathcal{N}_{neighbors_{\xi_{s_j}}}} X_k(t)$ denotes the total information ages when the mobile element j execute strategy s_j.

Thus, we can see that if the total residual energy at the meeting point is lower, the corresponding payoff will be higher. In addition, if the total information ages at the meeting point is higher, the payoff is higher. When the distance between the mobile element and the next meeting point is shorter, the payoff is higher. Therefore, by properly choosing the meeting point, the high profit obtains. Especially, when more than one mobile elements choose the same meeting point at the same decision-making process, we could use the game to make the visiting decision and avoid the conflict. Since the decision processes of trajectories are converted into repetitive games among mobile elements, we illustrate the game process for one round only, and this is shown in Algorithm 1.

C. CONFLICT AVOIDANCE
We take two players (m_1 and m_2) as an example to show the game process. The profits can be expressed as the payoff matrix P_{m_1, m_2} as:

$$\begin{bmatrix} P_{rs_1}^1, P_{rs_1}^2 & \cdots & P_{rs_1}^1, P_{rs_b}^2 & \cdots & P_{rs_1}^1, P_{rs_{\mathcal{N}_2'}}^2 \\ \vdots & \vdots & \vdots & \vdots & \vdots \\ P_{rs_a}^1, P_{rs_1}^2 & \cdots & P_{rs_a}^1, P_{rs_b}^2 & \cdots & P_{rs_a}^1, P_{rs_{\mathcal{N}_2'}}^2 \\ \vdots & \vdots & \vdots & \vdots & \vdots \\ P_{rs_{\mathcal{N}_1'}}^1, P_{rs_1}^2 & \cdots & P_{rs_{\mathcal{N}_1'}}^1, P_{rs_b}^2 & \cdots & P_{rs_{\mathcal{N}_1'}}^1, P_{rs_{\mathcal{N}_2'}}^2 \end{bmatrix}$$

where $P_{rs_a}^j$ indicates the profit of the mobile element j if it visits the requesting sensor node rs_a. $\mathcal{N}_1'$ and $\mathcal{N}_2'$

Algorithm 2 Queue for the Visiting Competition Within the Meeting Point

Input:
    $\mathcal{N}_{neighbors_\xi}$.
Output:
    The best strategy $\pi_j^{\xi*}$ for mobile element j.
1: **for** $k = 1; k \leq \mathcal{N}_{neighbors_\xi}; k++$ **do**
2:     $Q_j^\xi \leftarrow Q_j^\xi \cup \{k\}$;
3: **end for**
4: Sort the Q_j^ξ based on the residual energy of them;
5: **if** the mobile element j receives a new request from sensor node i when it is visting the meeting point ξ
    then
6:     $Q_j^{\xi'} \leftarrow Q_j^{\xi'} \cup \{i\}$;
7:     Sort the $Q_j^{\xi'}$ based on the residual energy of them;
8: **end if**
    return the best strategy $\pi_j^{\xi*}$.

---

denote the number of requests which are received by these two mobile elements at the same decision period, respectively.

In the game, each mobile element tends to choose a requesting sensor node that can obtain the maximum profits as the next meeting point. However, a conflict may happen when multiple mobile elements tend to visit the same requesting sensor node. In this case, to avoid the waste of time and energy, a sensor node can only be visited by only one mobile element for one request. The mobile element who can obtain the most payoff value from this sensor node can get access. To obtain the maximum total profits, other mobile elements choose the suboptimum sensor nodes as the meeting points in their strategy sets.

D. JUMP AND RE-QUEUEING
We define the requesting sensor nodes which are within the communication range of a meeting point are the neighbors of this meeting point. When a mobile element has chosen a meeting point and arrived at this point, all the neighbors of this meeting point will be visited. We design a jump and re-queueing time-slot allocation to schedule the mobile element to visit these neighbors. Notice that no matter how the scheme design, the AoI and energy efficiency could not be affected. This is because the time-slot allocation cannot change the request time and the arrival time of these neighbors' information. However, based on the residual energy of neighbors to schedule the access order of the mobile element, the shutdown period of the low energy neighbors can be shortened, and the successful visiting ratio can be improved. This process is shown in Algorithm 2.

If some new requests which are within the communication range of the meeting point send to the mobile element when the meeting point is being visited, the new requesting sensor nodes become the neighbors of this meeting point and will be visited by this mobile element at this round.

E. RETURN POLICY

In order to shorten the AoI of collected information, we design a return policy. The policy does not encourage the mobile element return after it tends to consume all the energy of itself. On the contrary, if one of the following conditions is satisfied, the mobile element returns.

- All the sensor nodes have been visited at this round.
- S_j is empty twice.
- The mobile element does not have enough energy to visit more sensor nodes.
- The travel time of the mobile element is equal or longer than the threshold.

F. ANALYSIS

In this section, we theoretically analyze the characteristic of the proposed scheme.

Lemma 1: In the network, the requests of sensor nodes for data transmission follow the poisson distribution.

Proof: The poisson distribution is popular for modeling the number of occurrence times of an event in an interval of time or space. In our model, whether a sensor node needs to send data is independent of other sensor nodes. The number of new requests in any given subinterval is independent of any other subinterval. We assume the probability of more than one request in a subinterval is very small. The probability of one request sending in a subinterval is proportional to the length of the subinterval. Thus, the number of requests for each interval follows the possion distribution, it can be shown as follows:

$$P(X = \mathcal{N}_r) = \frac{\lambda^{\mathcal{N}_r} e^{-\lambda}}{\mathcal{N}_r!}, \tag{20}$$

where λ is equal to the expected value of X and we have $\lambda = Np$. p denotes the probability of sending a request. $\mathcal{N}_r!$ is the factorial of $\mathcal{N}_r$. We use this equation to estimate the number of request $\mathcal{N}_r$ in each subinterval. □

Lemma 2: In the game, when a conflict exists, based on the rules of AMES, the outcome is pareto-optimal.

Proof: when more than one mobile element chooses the same one sensor node as the meeting point, the conflict happens. Based on the rules of the cooperative enforcement game, the mobile elements as the players, the target sensor node knowns all the payoff information of these players and enforce the player which can bring the maximum profits get access. The other players choose the suboptimal strategy of their strategy sets. The results of this game constitute a strategy profile s. If it is not pareto-optimal and the pareto-optimal strategy profile is s', the total payoff of s' should be greater than s. This is contradictory to the rules of the cooperative enforcement game. Therefore, when a conflict exists, the outcome of the game is pareto-optimal. □

Lemma 3: In the game, when a conflict does not exist, based on the rules of AMES, the outcome is pareto-optimal.

TABLE 2. Simulation parameters.

Parameters	Values
Number of Sensor Nodes	200
Number of Mobile Elements	10
Network size(m^2)	200×200
Energy capacity of sensor nodes(KJ)	1.08×10^3
Energy capacity of mobile elements(KJ)	2×10^6
$l(bit)$	10
Charging threshold of sensor nodes	20%
Moving cost of mobile elements per unit distance(J/m)	50
Moving speed of mobile elements (m/s)	0.5
$Eelec(nJ/bit)$	50
Communication radius of sensor nodes (m)	40
$c_s(nJ/s)$	1
$\varepsilon fs(PJ/bit/m^\alpha)$	10

Proof: If there is no conflict in the game, each mobile element chooses the maximum payoff strategy and these choices constitute a strategy profile s. In this condition, no one has the possibility to obtain another strategy that any of players can obtain more profits than it can obtain by strategy profile s.

Thus, when a conflict does not exist, based on the rules of AMES, the outcome of the game is pareto-optimal. □

In summary, whether or not a conflict exists in the game process, the outcome of AMES is pareto-optimal.

IV. PERFORMANCE EVALUATION

In this section, the performance of AMES is evaluated and compared with the existing approaches through extensive simulations.

A. SIMULATION SETUP

The parameters used in the simulations are listed in Table 2. In our simulation, we consider 200 sensor nodes randomly scattered over a 200×200 square meters area. The sink point is located at (300, 200). 10 mobile elements depart from the sink point with full charged battery and return when they follow the return policy of AMES. We assume the mobile elements move at a speed of $0.5m/s$ with the traveling cost rate $50J/s$. The battery capacity of a mobile element is $E^m = 2 \times 10^6$ J. The battery capacity of a sensor node is $E^s = 1.08 \times 10^3$ J and the path loss exponent is $\alpha = 2$. The communication radius of a sensor node is $40m$. When the energy of a sensor node is less than 20 percent of its battery capacity, the sensor node sends a charging request. The effective receiving power is $\varepsilon fs = 10 \ PJ/bit/m^\alpha$ and $E_{elec} = 50 \ nJ/bit$. The sensing energy consumption rate is $1 \ nJ/s$.

We compare our scheme with GA based scheme when different reasonable parameters are adopted. GA is a classic trajectory scheduling algorithm, which chooses the meeting point with the minimum distance between the meeting point and the mobile element in each meeting point decision. In order to verify the effects of the neighborhood, we extend our scheme to an AMES-neighborless, in which the mobile elements only visit the sensor nodes which are at the meeting points. GA is also extended to a GA-neighborhood scheme
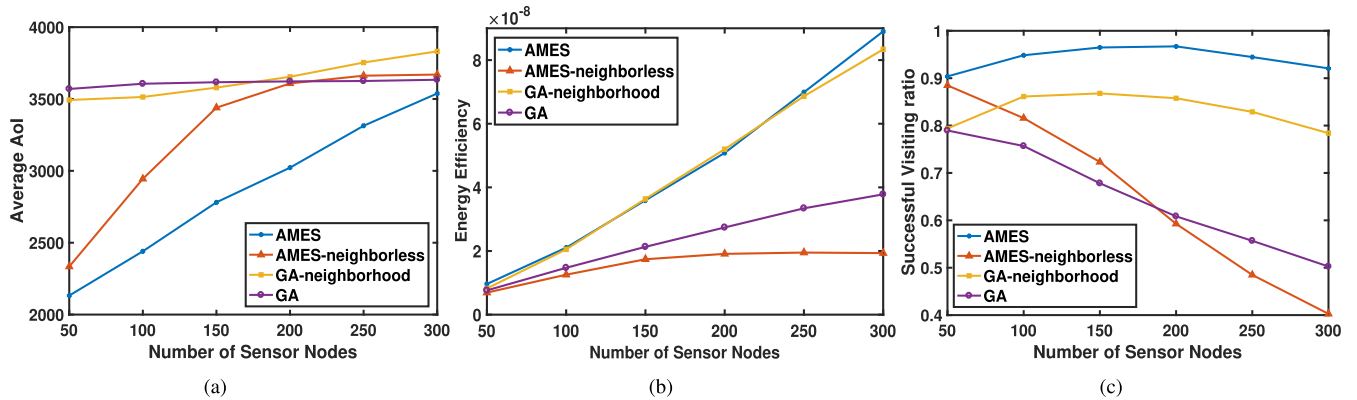
FIGURE 4. Performance comparison between AMES,AMES-Neighborless, GA, GA-Neighborhood with the different number of sensor nodes in terms of (a) average AoI, (b) energy efficiency, (c) successful visiting ratio.
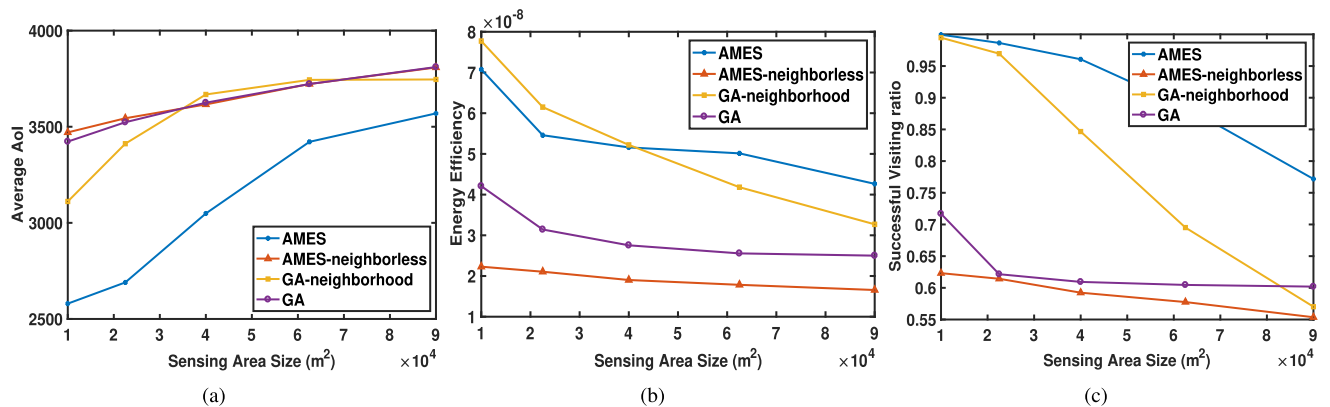

FIGURE 5. Performance comparison between AMES,AMES-Neighborless, GA, GA-Neighborhood with the different sizes of sensing area in terms of (a) average AoI, (b) energy efficiency, (c) successful visiting ratio.

to future verify this. All results are the average of 100 runs of simulations.

B. IMPACT OF NETWORK SCALE

To investigate the scalability of AMES, we evaluate the performance with different network scales w.r.t the size of the sensing area and the number of deployed sensor nodes. Based on the different number of sensor nodes, the resultant average AoI, energy efficiency and successful visiting ratio are shown in Figure 4. We can see AMES achieves the best average AoI and successful visiting ratio. With the increasing of the number of sensor nodes, the average AoI increases until it reaches the return threshold. Comparing to AMES, both the average AoI of GA and GA-neighborhood maintain on the return threshold. This mean the mobile elements return until the return threshold is reached. Even though GA and GA-neighborhood spent more time to collect information, the successful visiting ratio is lower than AMES. Besides, increasing the number of sensor nodes, the energy efficiency increases, and AMES obtains the best energy efficiency when it exceeds 200.

Fixing the number of sensor nodes 200, we evaluate the performance of AMES with varying the length of the side of the sensing area from 100 to 300, as shown in Figure 5. Due to the limited communication radius, the number of

the received requests and the successful visiting ratio are decreased with the increasing of the size of the sensing area. AMES achieves the best energy efficiency when the sensing area size is more than 40000 square meters, and the average AoI and the successful visiting ratio of AMES are always better than the other schemes in the figure.

C. IMPACT OF THE NUMBER OF MOBILE ELEMENTS

An important factor determines the visiting ability in performing visiting tasks is the number of mobile elements. With the number of mobile elements varying from 2 to 20, we evaluate the average AoI, energy efficiency and successful visiting ratio in Figure 6. As all the mobile elements depart from the sink point, travel in the network and return to the same sink point, increasing the number of mobile elements may lead to a reduction of energy efficiency, as shown in Figure 6(b). However, in this case, the average AoI obviously decreases, and the successful visiting ratio increases to nearly 1. Although a mobile element only visits a sensor node that can obtain a small average AoI, the other two performance and the mobile element utilization are low. Thus, the trajectories scheduling of multiple mobile elements has a great influence on these performances and AMES has its advantages.
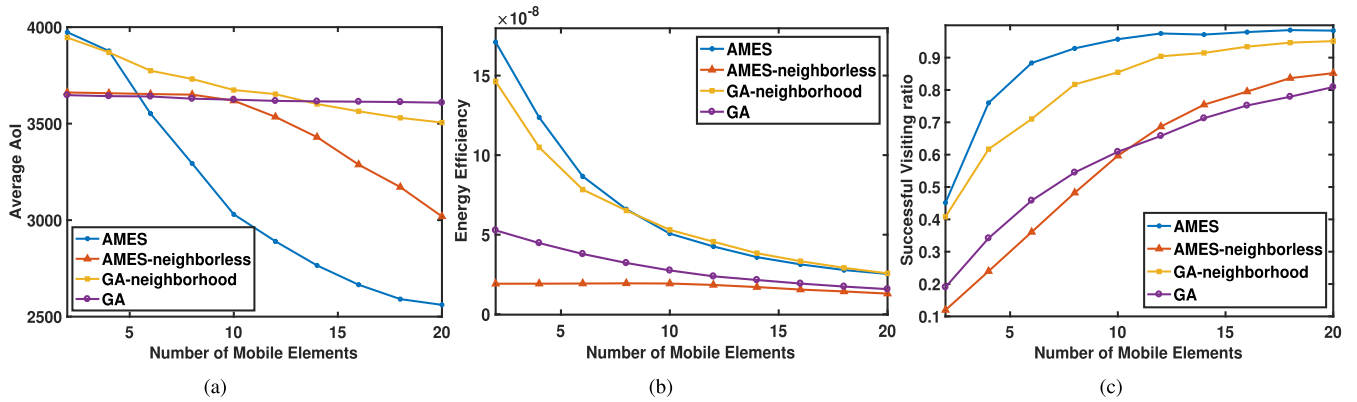
FIGURE 6. Performance comparison between AMES, AMES-Neighborless, GA, GA-Neighborhood with the different number of mobile elements in terms of (a) average AoI, (b) energy efficiency, (c) successful visiting ratio.
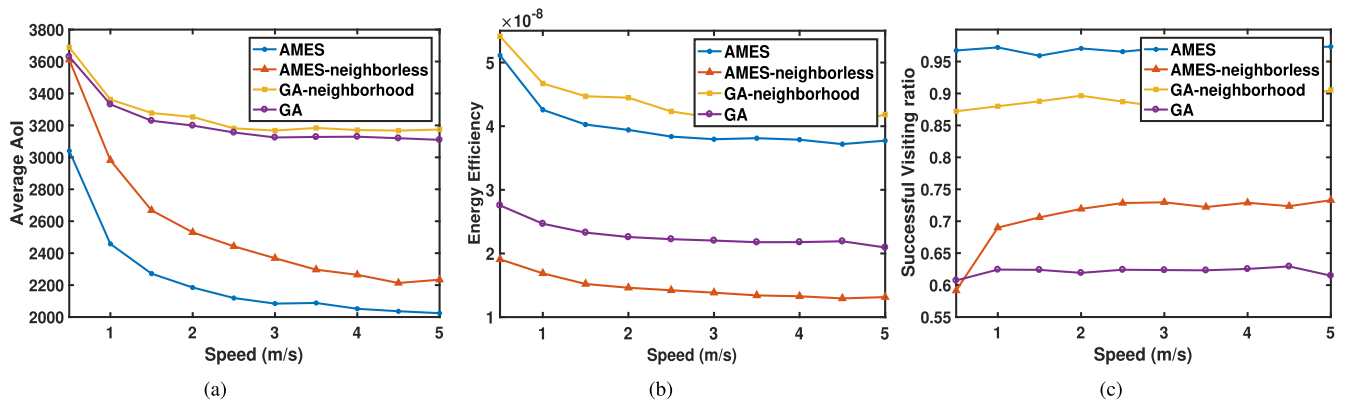

FIGURE 7. Performance comparison between AMES, AMES-Neighborless, GA, GA-Neighborhood with the different travel speeds of mobile elements in terms of (a) average AoI, (b) energy efficiency, (c) successful visiting ratio.
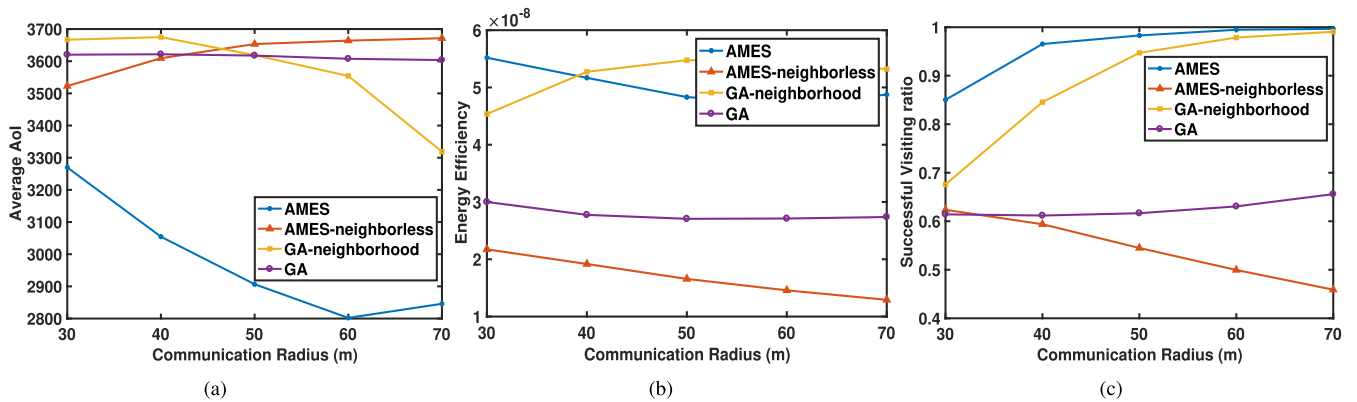

FIGURE 8. Performance comparison between AMES, AMES-Neighborless, GA, GA-Neighborhood with the different sizes of communication radius in terms of (a) average AoI, (b) energy efficiency, (c) successful visiting ratio.

D. IMPACT OF THE TRAVEL SPEED OF MOBILE ELEMENTS

Another factor affects the mobile element's ability in performing visiting tasks is its travel speed. We explore the performance of AMES with varying travel speed from $0.5 m/s$ to $5 m/s$. The resultant average AoI, energy efficiency and successful visiting ratio are shown in Figure 7. It can be seen that increasing the travel speed of the mobile element can reduce the average AoI. The advantage of the average AoI of AMES can be clearly observed. Although increasing

the travel speed has little effect on the energy efficiency and successful visiting ratio, the successful visiting ratio of AMES is obviously higher than the other three schemes.

E. IMPACT OF THE SIZE OF COMMUNICATION RANGE

To future investigate the performance of AMES, we evaluate and analyze the impact of the size of the communication radius on the original problem in this section. With the communication radius varying from 30 to 70 meters,

the evaluation results on the average AoI, energy efficiency and successful visiting ratio are shown in Figure 8. The size of the communication radius affects the number of the received requests. Although the energy efficiency has some declines because of the charging and transmission path loss in Figure 8(b), we can see that the advantage of average AoI of AMES obviously increases with the increasing of the requesting sensor nodes within the communication range until the communication radius is greater than 60 in Figure 8(a). In Figure 8(c), the successful visiting ratio of AMES is increased with the increasing of the size of the communication radius. When the communication radius is longer than 60, the successful visiting ratio of AMES is nearly 1. Thus, in this case, the average AoI of AMES tends to be stable.

V. CONCLUSION

This paper mainly focused on the mobile elements scheduling problem and formulated a multi-objective optimization to minimize the average AoI and maximum the energy efficiency for multiple independent and rechargeable sensors network in green IoT. Based on the design of the cooperative enforcement game, AMES scheme was proposed to schedule the trajectories of mobile elements to solve this problem. By obeying the rules of the game, the conflicts are avoided between the mobile elements, and the outcome of the game is pareto-optimal. We evaluated and compared the proposed scheme by extensive simulations. The results showed that the performance of the average AoI, the energy efficiency and the successful visiting ratio have been improved significantly.

REFERENCES

[1] Z. W. Siew, Y. K. Chin, A. Kiring, H. P. Yoong, and K. T. K. Teo, "Comparative study of various cluster formation algorithms in wireless sensor networks," in *Proc. 7th Int. Conf. Comput. Converg. Technol. (ICCCT)*, Seoul, South Korea, Dec. 2012, pp. 772–777.

[2] T. Watteyne, A. Molinaro, M. G. Richichi, and M. Dohler, "From MANET to IETF ROLL standardization: A paradigm shift in WSN routing protocols," *IEEE Commun. Surveys Tuts.*, vol. 13, no. 4, pp. 688–707, 4th Quart., 2011.

[3] S. Li, H. Shen, Q. Huang, and L. Guo, "Optimizing the sensor movement for barrier coverage in a sink-based deployed mobile sensor network," *IEEE Access*, vol. 7, pp. 156301–156314, 2019.

[4] D. Zhang, Z. Chen, M. K. Awad, N. Zhang, H. Zhou, and X. S. Shen, "Utility-optimal resource management and allocation algorithm for energy harvesting cognitive radio sensor networks," *IEEE J. Sel. Areas Commun.*, vol. 34, no. 12, pp. 3552–3565, Dec. 2016.

[5] D. Zhang, Z. Chen, J. Ren, N. Zhang, M. K. Awad, H. Zhou, and X. S. Shen, "Energy-Harvesting-Aided spectrum sensing and data transmission in heterogeneous cognitive radio sensor network," *IEEE Trans. Veh. Technol.*, vol. 66, no. 1, pp. 831–843, Jan. 2017.

[6] L. Fu, P. Cheng, Y. Gu, J. Chen, and T. He, "Optimal charging in wireless rechargeable sensor networks," *IEEE Trans. Veh. Technol.*, vol. 65, no. 1, pp. 278–291, Jan. 2016.

[7] M. Abo-Zahhad, S. M. Ahmed, N. Sabor, and S. Sasaki, "Mobile sink-based adaptive immune energy-efficient clustering protocol for improving the lifetime and stability period of wireless sensor networks," *IEEE Sensors J.*, vol. 15, no. 8, pp. 4576–4586, Aug. 2015.

[8] X. Zha, W. Ni, X. Wang, R. P. Liu, Y. J. Guo, X. Niu, and K. Zheng, "The impact of link duration on the integrity of distributed mobile networks," *IEEE Trans. Inf. Forensics Security*, vol. 13, no. 9, pp. 2240–2255, Sep. 2018.

[9] R. Pozza, M. Nati, S. Georgoulas, K. Moessner, and A. Gluhak, "Neighbor discovery for opportunistic networking in Internet of Things scenarios: A survey," *IEEE Access*, vol. 3, pp. 1101–1131, 2015.

[10] H. Huang, S. Guo, W. Liang, K. Wang, and A. Y. Zomaya, "Green data-collection from geo-distributed IoT networks through low-earth-orbit satellites," *IEEE Trans. Green Commun. Netw.*, vol. 3, no. 3, pp. 806–816, Sep. 2019.

[11] I. Kadota, A. Sinha, and E. Modiano, "Scheduling algorithms for optimizing age of information in wireless networks with throughput constraints," *IEEE/ACM Trans. Netw.*, vol. 27, no. 4, pp. 1359–1372, Aug. 2019.

[12] Y.-P. Hsu, E. Modiano, and L. Duan, "Scheduling algorithms for minimizing age of information in wireless broadcast networks with random arrivals," *IEEE Trans. Mobile Comput.*, early access, Aug. 20, 2019, doi: 10.1109/TMC.2019.2936199.

[13] I. Kadota, A. Sinha, E. Uysal-Biyikoglu, R. Singh, and E. Modiano, "Scheduling policies for minimizing age of information in broadcast wireless networks," *IEEE/ACM Trans. Netw.*, vol. 26, no. 6, pp. 2637–2650, Dec. 2018.

[14] B. Zhou and W. Saad, "Optimal sampling and updating for minimizing age of information in the Internet of Things," in *Proc. IEEE Global Commun. Conf. (GLOBECOM)*, Abu Dhabi, UAE, Dec. 2018, pp. 1–6.

[15] B. Buyukates, A. Soysal, and S. Ulukus, "Age of information in multihop multicast networks," *J. Commun. Netw.*, vol. 21, no. 3, pp. 256–267, Jun. 2019.

[16] A. M. Bedewy, Y. Sun, and N. B. Shroff, "The age of information in multihop networks," *IEEE/ACM Trans. Netw.*, vol. 27, no. 3, pp. 1248–1257, Jun. 2019.

[17] I. Krikidis, "Average age of information in wireless powered sensor networks," *IEEE Wireless Commun. Lett.*, vol. 8, no. 2, pp. 628–631, Apr. 2019.

[18] E. T. Ceran, D. Gündüz, and A. György, "Reinforcement learning to minimize age of information with an energy harvesting sensor with HARQ and sensing cost," 2019, *arXiv:1902.09467*. [Online]. Available: http://arxiv.org/abs/1902.09467

[19] Z. Zhou, C. Du, L. Shu, G. Hancke, J. Niu, and H. Ning, "An energy-balanced heuristic for mobile sink scheduling in hybrid WSNs," *IEEE Trans. Ind. Informat.*, vol. 12, no. 1, pp. 28–40, Feb. 2016.

[20] M. Samir, S. Sharafeddine, C. M. Assi, T. M. Nguyen, and A. Ghrayeb, "UAV trajectory planning for data collection from time-constrained IoT devices," *IEEE Trans. Wireless Commun.*, vol. 19, no. 1, pp. 34–46, Jan. 2020.

[21] W. Yang, Y. Zhang, C. Yang, Z. Zuo, and X. Wang, "Online power scheduling for distributed filtering over an energy-limited sensor network," *IEEE Trans. Ind. Electron.*, vol. 65, no. 5, pp. 4216–4226, May 2018.

[22] A. Arafa, J. Yang, and S. Ulukus, "Age-minimal online policies for energy harvesting sensors with random battery recharges," in *Proc. IEEE Int. Conf. Commun. (ICC)*, Kansas City, MO, USA, May 2018, pp. 1–6.

[23] P. Zhong, Y. Zhang, S. Ma, X. Kui, and J. Gao, "RCSS: A real-time on-demand charging scheduling scheme for wireless rechargeable sensor networks," *Sensors*, vol. 18, no. 5, p. 1601, 2018.

[24] C. Lin, J. Zhou, C. Guo, H. Song, G. Wu, and M. S. Obaidat, "TSCA: A temporal-spatial real-time charging scheduling algorithm for on-demand architecture in wireless rechargeable sensor networks," *IEEE Trans. Mobile Comput.*, vol. 17, no. 1, pp. 211–224, Jan. 2018.

[25] C. Lin, S. Wei, J. Deng, M. S. Obaidat, H. Song, L. Wang, and G. Wu, "GTCCS: A game theoretical collaborative charging scheduling for on-demand charging architecture," *IEEE Trans. Veh. Technol.*, vol. 67, no. 12, pp. 12124–12136, Dec. 2018.

[26] A. Kaswan, A. Tomar, and P. K. Jana, "An efficient scheduling scheme for mobile charger in on-demand wireless rechargeable sensor networks," *J. Netw. Comput. Appl.*, vol. 114, pp. 123–134, Jul. 2018.

[27] M. Hua, Y. Wang, Z. Zhang, C. Li, Y. Huang, and L. Yang, "Power-efficient communication in UAV-aided wireless sensor networks," *IEEE Commun. Lett.*, vol. 22, no. 6, pp. 1264–1267, Jun. 2018.

[28] J. Liu, X. Wang, B. Bai, and H. Dai, "Age-optimal trajectory planning for UAV-assisted data collection," in *Proc. IEEE Conf. Comput. Commun. Workshops (INFOCOM WKSHPS)*, Apr. 2018, pp. 553–558.

[29] K. Wang, Z. Chu, Y. Zhou, K. Wang, C. Lin, and M. S. Obaidat, "Partial charging scheduling in wireless rechargeable sensor networks," in *Proc. IEEE Global Commun. Conf. (GLOBECOM)*, Abu Dhabi, UAE, Dec. 2018, pp. 1–6.

[30] A. Y. Wang and C. G. Sodini, "A simple energy model for wireless microsensor transceivers," in *Proc. IEEE Global Telecommun. Conf. (GLOBECOM)*, Dallas, TX, USA, Nov. 2004, pp. 3205–3209.

[31] W. B. Heinzelman, A. P. Chandrakasan, and H. Balakrishnan, "An application-specific protocol architecture for wireless microsensor networks," *IEEE Trans. Wireless Commun.*, vol. 1, no. 4, pp. 660–670, Oct. 2002.

JIANXIN MA received the M.S. degree in integrated circuit engineering from the Harbin Institute of Technology (HIT), China, in 2013, where she is currently pursuing the Ph.D. degree in information and communication engineering. Her research interests include data gathering algorithm, age of information, and wireless sensor networks.

SHUO SHI (Member, IEEE) received the M.S. and Ph.D. degrees in information and communication engineering from the Harbin Institute of Technology (HIT), Harbin, China, in 2004 and 2008, respectively. He studied as an Exchange Student with the Network Research Laboratory, Sungkyunkwan University, South Korea, from 2004 to 2005. He is currently an Associate Professor with the Communication Research Center, HIT. His research interests include mobile wireless ad-hoc networks, signal detection, and network architecture research of space vehicle.
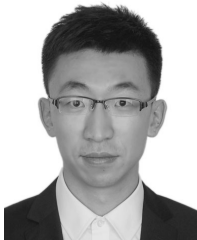
SHUSHI GU (Member, IEEE) received the M.S. and Ph.D. degrees in information and communication engineering from the Harbin Institute of Technology, in 2012 and 2016, respectively. From 2016 to 2019, he was a Postdoctoral Research Fellow with the Harbin Institute of Technology (Shenzhen), Shenzhen, China. From 2018 to 2019, he was a Postdoctoral Research Fellow and a Visiting Scholar with James Cook University, Cairns, Australia. He is currently an Assistant Professor with the School of Electronic and Information Engineering, HITSZ. His current research interests include the satellite IoT, coding theory, edge caching, and distributed storage. He received the Best Paper Awards of IEEE WCSP 2015 and EAI WiSATS 2019. He received the Outstanding Postdoctoral Award of HITSZ, in 2018.

NING ZHANG (Senior Member, IEEE) received the Ph.D. degree from the University of Waterloo, Canada, in 2015.

He was a Postdoctoral Research Fellow with the University of Waterloo and the University of Toronto, Canada. His current research interests include next generation mobile networks, physical layer security, machine learning, and mobile edge computing. He serves/served as an Associate Editor of the IEEE TRANSACTIONS ON COGNITIVE COMMUNICATIONS AND NETWORKING, IEEE ACCESS, and *IET Communications*, an Area Editor of the *Encyclopedia of Wireless Networks* (Springer and Cambridge Scholars), and a Guest Editor of *Wireless Communication and Mobile Computing*, the *International Journal of Distributed Sensor Networks*, and *Mobile Information System*.

XUEMAI GU received the M.S. and Ph.D. degrees from the Department of Information and Communication Engineering, Harbin Institute of Technology (HIT), in 1985 and 1991, respectively. He is currently a Professor and the President of the Graduate School of HIT. His research interests focus on integrated and hybrid satellite-terrestrial communications and broadband multimedia communication technique.

● ● ●